

THE PROGENITOR OF SN 2011JA: CLUES FROM CIRCUMSTELLAR INTERACTION

SAYAN CHAKRABORTI¹

Institute for Theory and Computation, Harvard-Smithsonian Center for Astrophysics, 60 Garden Street, Cambridge, MA 02138, USA

ALAK RAY

Tata Institute of Fundamental Research, 1 Homi Bhabha Road, Colaba, Mumbai 400 005, India

RANDALL SMITH

Harvard-Smithsonian Center for Astrophysics, 60 Garden Street, Cambridge, MA 02138, USA

STUART RYDER

Australian Astronomical Observatory, P.O. Box 915, North Ryde, NSW 1670, Australia

NAVEEN YADAV

Tata Institute of Fundamental Research, 1 Homi Bhabha Road, Colaba, Mumbai 400 005, India

FIROZA SUTARIA

Indian Institute of Astrophysics, Koramangala, Bangalore, India

VIKRAM V. DWARKADAS

Department of Astronomy and Astrophysics, University of Chicago, 5640 S Ellis Avenue, Chicago, IL 60637, USA

POONAM CHANDRA

Department of Physics, Royal Military College of Canada, Kingston, ON, K7K 7B4, Canada

DAVID POOLEY

Department of Physics, Sam Houston State University, Huntsville, TX, USA

RUPAK ROY

Aryabhata Research Institute of Observational Sciences, Manora peak, Nainital, India

DRAFT September 20, 2018

ABSTRACT

Massive stars, possibly red supergiants, which retain extended hydrogen envelopes until core collapse, produce Type II Plateau (IIP) supernovae. The ejecta from these explosions shock the circumstellar matter originating from the mass loss of the progenitor during the final phases of its life. This interaction accelerates particles to relativistic energies which then lose energy via synchrotron radiation in the shock-amplified magnetic fields and inverse Compton scattering against optical photons from the supernova. These processes produce different signatures in the radio and X-ray part of the electromagnetic spectrum. Observed together, they allow us to break the degeneracy between shock acceleration and magnetic field amplification. In this work we use X-rays observations from the Chandra and radio observations from the ATCA to study the relative importance of processes which accelerate particles and those which amplify magnetic fields in producing the non-thermal radiation from SN 2011ja. We use radio observations to constrain the explosion date. Multiple Chandra observations allow us to probe the history of variable mass loss from the progenitor. The ejecta expands into a low density bubble followed by interaction with a higher density wind from a red supergiant consistent with $\dot{M}_{\text{ZAMS}} \gtrsim 16M_{\odot}$. Our results suggest that a fraction of type IIP supernovae may interact with circumstellar media set up by non-steady winds.

Subject headings: Stars: Mass Loss — Supernovae: Individual: SN 2011ja — shock waves — circumstellar matter — radio continuum: general — X-rays: general

1. INTRODUCTION

Type IIP supernovae display prominent P Cygni features around the time of peak luminosity, produced by hydrogen lines and their optical light curve plateaus for ~ 100 days in the rest-frame of the supernova (Doggett & Branch 1985; Arcavi et al. 2012). This characteristic phase in their optical light curves is attributed to their progenitors retaining extended hydrogen envelopes until the time of core collapse. Popov (1993) found that the duration of the plateau phase has a strong dependence on the mass of the hydrogen envelope and weak dependence on the explosion energy and the initial radius. These lines of evidence and direct pre-explosion imaging (Smartt et al. 2009) suggest that these stars exploded as red supergiants. Smartt et al. (2009) found that two-thirds of the core collapse supernovae in their sample, volume limited to $d < 30$ Mpc, are type IIP. Smith et al. (2011) estimate the fraction to be closer to half.

Red supergiants have been found inside the Local Group with masses up to $25 M_{\odot}$, but Smartt et al. (2009) did not find any red supergiants with masses greater than $17 M_{\odot}$ as progenitors of type IIP supernovae. Many solutions have been suggested for the *red supergiant problem*. O’Connor & Ott (2011) have suggested that the zero-age main sequence (ZAMS) mass, metallicity, rotation and mass-loss prescription controls the compactness of the stellar core at bounce which determines whether a core-collapse supernova will fail and instead form a stellar-mass black hole. Walmswell & Eldridge (2012) have suggested circumstellar dust as a solution to the problem of the missing massive progenitors. In this situation, understanding the nature, amount and variability of mass loss from the progenitors of type IIP supernovae is crucial for resolving this puzzle.

The ejecta from these explosions shocks the circumstellar matter set up by the mass loss of the progenitor during the final phases of its life. Since the ejecta ($\sim 10^4$ km s $^{-1}$) moves about a thousand times faster than the stellar wind (~ 10 km s $^{-1}$), this expanding ejecta probes a millennium of red supergiant mass loss history in a year, a timescale which would otherwise be inaccessible in human lifetimes. This interaction accelerates particles to relativistic energies, which then lose energy via synchrotron radiation in the shock-amplified magnetic fields and inverse Compton scattering against optical photons from the supernova. Chevalier et al. (2006) have shown that these processes produce separate signatures in the radio and X-ray part of the electromagnetic spectrum. Chakraborti et al. (2012) have demonstrated that combining radio and X-ray spectra allows one to break the degeneracy between the efficiencies of shock acceleration and field amplification. In this work we use X-rays observations from Chandra and radio observations from the Australia Telescope Compact Array (ATCA) to study the relative importance of particle acceleration and magnetic field amplification for producing the non thermal radiation from SN 2011ja. Dwarkadas & Gruszko (2012) have indicated that the expansion and density structure of the circumstellar matter must be investigated before assumptions can be made of steady wind expansion. It has been shown that the X-ray observations of SN 2004dj suggest variable mass loss though they do not rule out

TABLE 1
OBSERVATION OF SN 2011JA WITH CHANDRA

Date	XB Flux (0.3-10 keV) (10^{-14} ergs cm $^{-2}$ s $^{-1}$)	SN Flux (0.3-10 keV) (10^{-14} ergs cm $^{-2}$ s $^{-1}$)
2000 Jan 27	1.01 ± 0.11	none
2012 Jan 10	0.81 ± 0.10	0.98 ± 0.17
2012 Apr 03	1.01 ± 0.11	4.08 ± 0.42

NOTE. — Fluxes are model dependent. X-ray binary is modelled as tbabs(diskbb) and supernova is modeled as tbabs(powerlaw) in XSPEC. See subsection 3.1 for details. Fluxes reported in this table are from the full model and not corrected for absorption.

a constant mass-loss scenario (Chakraborti et al. 2012). In this work we use a multiple Chandra observation of SN 2011ja to establish variable mass loss from the progenitor.

2. OBSERVATIONS OF SN 2011JA

SN 2011ja occurred in the nearby galaxy NGC 4945 at a distance of 3.36 ± 0.09 Mpc (Mouhcine et al. 2005). The supernova was first reported in Monard et al. (2011) where it was noted that Monard observed the SN at 14.0 magnitude (unfiltered CCD) on December 18.1 UT and Milisavljevic obtained a spectrum on December 19.1 UT that matched the type IIP SN 2004et about a week after maximum light. For SN 2004et Crockett et al. (2011) have used the difference between the pre and post-explosion, ground-based observations to deduce a progenitor mass of $\sim 8 M_{\odot}$. Jerkstrand et al. (2012) have found a progenitor mass of $\sim 15 M_{\odot}$ for SN 2004et from late-time spectral modeling while Sahu et al. (2006) had found $\sim 15 M_{\odot}$ from light-curve modelling. We commenced our multi-wavelength campaign following the discovery of SN 2011ja. Our observations in X-rays and radio, reported and used in this work, are described in detail below.

2.1. Chandra X-ray Observations

SN 2011ja was observed by a Target of Opportunity proposal (PI: Ray, Cycle: 13, ObsID: 13791) on 2012 January 10 and subsequently using Director’s Discretionary Time (ObsID: 14412) on 2012 April 03 from the *Chandra X-ray Observatory*. were used on both occasions, without any grating, for 40 ks each. The supernova was clearly detected in both of these observations. We also analyzed a pre-explosion 50 ks observation of the field (PI: Madejski, Cycle: 1, ObsID: 864) to look for possible contamination. Details of our observations are listed in Table 1.

Before spatial and spectral analysis, we processed the data from different epochs separately but identically. We followed the prescription from the Chandra Science Center using CIAO 4.4 with CALDB 4.4.8. We filtered the level 2 events in energy to only select ones between 0.3 keV and 10 keV. The selected events were projected on the sky and the region of interest (a box with 20” sides, centered on the optical supernova position) was identified. We masked the region of interest and generated a light curve from the remaining counts. We used this background light curve to identify flaring and further masked time-ranges where the background count rate was greater than 3 times the rms. This left us with a table of good time intervals which was then used to select the reliable events. The steps followed up to here are

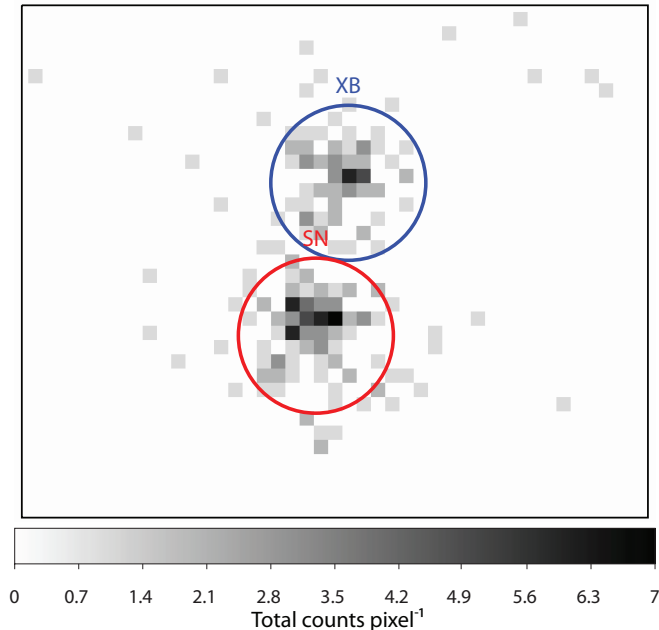


FIG. 1.— Photon counts obtained in the last Chandra epoch. The filtered Chandra events have been binned into image pixels which have 0.25 ACIS pixel sides. Note the spectral extraction regions for SN 2011ja (lower left in red) and contaminating X-ray binary (upper right in blue).

the same as followed in Chakraborti et al. (2012). The pre-explosion observation revealed the presence of a contaminating source 1.35" from the supernova.

The spectrum of the contaminating source was extracted and it seems to be an X-ray binary. We shall explore the nature of this source in an upcoming work. However, the contaminant could not be precisely localized in the pre-SN exposure as it was 4.6' away from Chandra's bore-sight, where the PSF degradation is substantial. Thus, detailed analysis of the post explosion observations were required in order to separate the supernova's flux from that of the contamination. We fit, using Sherpa, the 2-D image created from the event file of each observation by binning over the region of interest in 0.25 ACIS pixel sizes (See Figure 1). We also created a PSF image file to use as a template using the CIAO tool `mkpsf`, which extracts a PSF model image from a given standard PSF library hypercube given an energy, offset and sky or detector physical coordinates. A source model of two point sources and a fixed background, convolved with the appropriate PSF was then fitted to the image. This allowed us to determine the relative positions of the supernova and the contaminating source (just 1.35" away) which are found with sub-pixel accuracy in the image plane. The extraction regions were defined as circles with radius 0.67" centered at these positions. Given that these sources are on axis in the ToO observation, this area should contain $\sim 90\%$ of the flux. However, we have applied an energy-dependent point-source aperture correction, using the CIAO tool `arccorr`, to account for any missing flux. We generated the spectra, response and background files separately for both sources. We did not bin the data over energy and instead used unbinned data for further analysis to fully exploit the spectral resolution of the instrument.

TABLE 2
ATCA OBSERVATIONS SN 2011JA

Date	Frequency (GHz)	Flux Density (mJy)
2011 Dec 19	18.0	0.53 ± 0.09
2011 Dec 20	9.0	0.85 ± 0.11
2011 Dec 20	5.5	0.54 ± 0.10
2012 Apr 11	9.0	< 2.1

2.2. ATCA Radio Observations

SN 2011ja was observed in the radio soon after discovery with the ATCA (Ryder et al. 2011) and the Giant Metrewave Radio Telescope (GMRT) (Yadav & Chakraborti 2012). Table 2 lists the flux densities observed (or upper limit) with the ATCA using the Compact Array Broad-band Backend (CABB; Wilson et al. 2011) which provides 2×2 GHz IF bands. Total time on-source ranged from 1 to 2 hours, yielding sufficient uv-coverage to comfortably separate SN 2011ja from the side-lobes of the radio-bright nucleus of NGC 4945 some 250" to the northeast. The ATCA primary flux calibrator, PKS B1934-638 has been observed once per run at each frequency to set the flux scale at all frequencies. It also defined the bandpass calibration in each band, except for 18 GHz where the brighter source PKS B1253-055 was used instead. Frequent observations of the nearby source PKS B1320-446 allowed us to monitor and correct for variations in gain and phase during each run, and to update the antenna pointing model at 18 GHz. The data were edited and calibrated using standard tasks in the MIRIAD package (Sault et al. 1995), and images made using robust weighting. Fluxes in Table 2 were derived using the `uvfit` task to minimize uncertainties introduced by cleaning, phase stability, etc while fitting in the image plane, and the uncertainties calculated in the same manner as Weiler et al. (2011). An upper limit of 3 mJy (3σ) was obtained using GMRT observation on 2012 January 11 UT at an effective frequency of 1264 MHz.

3. NON-THERMAL EMISSION

The fast moving supernova ejecta shocks the slowly moving pre-explosion circumstellar matter set up by the stellar wind of the progenitor (Chevalier 1982). In a type IIP supernova, (Chakraborti et al. 2012) point out that the post forward shock circumstellar matter is at too high temperature and low density to produce a significant thermal contribution to the Chandra flux. However non-thermal electrons accelerated at the forward shock can produce most of the radio emission seen in type IIP supernovae (Chevalier et al. 2006). Either thermal (Sutaria et al. 2003) or non-thermal (Björnsson & Fransson 2004) electrons can Inverse Compton scatter a fraction of the optical supernova photons into the Chandra X-ray band. A non-thermal electron population specified by an index p produces synchrotron emission in radio with spectral index $(p - 1)/2$ and inverse Compton scattered X-rays with photon index $(p + 1)/2$.

3.1. X-ray Spectral Fitting

The supernova spectra were imported into XSPEC 12.7.1 for spectral analysis. Spectra from both epochs

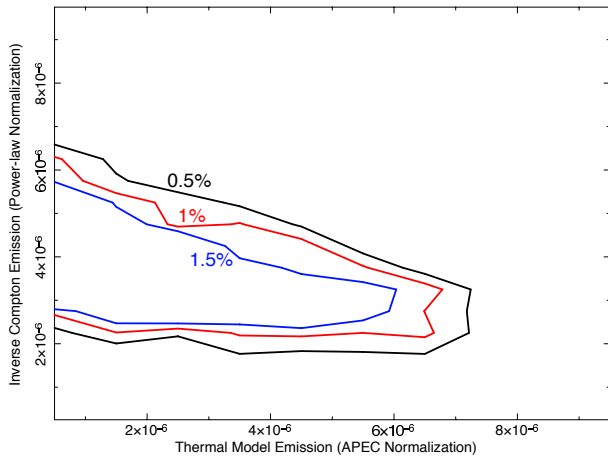


FIG. 2.— Probability density contours for models fitted to the Chandra data. Thermal flux (APEC normalization) on x-axis and inverse Compton flux (powerlaw normalization) on the y-axis. The thermal and inverse Compton fluxes are anti-correlated as their sum has to account for the combined flux observed with Chandra. Note however that the data does not rule out a zero thermal flux.

were fitted simultaneously with the sum of a non-thermal inverse Compton component using *powerlaw* and thermal emission from a collisionally-ionized diffuse gas using *APEC* models (Smith et al. 2001). The spectra was attenuated by a Tuebingen-Boulder (tbabs in XSPEC) ISM absorption model (Wilms et al. 2000). Moriya (2012) has shown that if the circumstellar medium is dense enough, collisional ionization equilibrium can be established in the early stage of the evolution of the supernova remnant, especially in the reverse shocked plasma (Chakraborti et al. 2012). The APEC plasma temperature was fixed at 1 keV as suggested by the temperature of the reverse-shocked material calculated by Nymark et al. (2006) and demonstrated to be appropriate for type IIP supernovae by Chakraborti et al. (2012). The powerlaw photon index representing the inverse Compton component was fixed at 2, as observed by Chakraborti et al. (2012) corresponding to $p = 3$. The column density for absorption was kept free but pegged to be same at both epochs. The APEC emission measure and powerlaw normalization were solved for both epochs from this joint analysis. Each spectral channel would have too few photons for a useful χ^2 estimation because the fits were performed on unbinned data. So we used the (Cash 1979) statistic to perform our fits.

In order to determine if the free parameters were indeed well constrained by the data, we ran Markov chain Monte Carlo (MCMC) simulations with 10000 steps over the multidimensional space of all the free parameters. We show in Fig 2 that while the inverse Compton component is well-detected, there is no conclusive evidence for the thermal plasma component. It has already been predicted (Chevalier et al. 2006) and observed (Chakraborti et al. 2012) that in type IIP supernovae the early X-ray emission is dominated by the inverse Compton component. Therefore for simplicity, we set the thermal flux to zero in the subsequent analysis. We generated 10000 simulated spectra for the best fit model to test its goodness of fit. $\sim 50\%$ of these spectra were found to have cstat less than that for the real data. This leads us to conclude that our best fit model provides a good fit to the data. The absorption column density

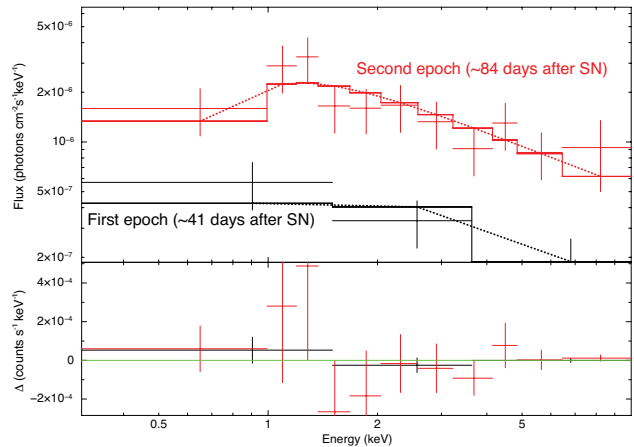


FIG. 3.— X-ray spectra of SN 2011ja. Bars are counts from Chandra, binned for display. Dotted line is the powerlaw model for the inverse Compton flux. Solid line is the full model after absorption, and binning. Black is first epoch (January 10) and red is second epoch (April 03). Note the significant increase in flux for the second epoch.

for the best fit model is $N_{\text{H}} = (7.5 \pm 0.9) \times 10^{21} \text{ cm}^{-2}$. Refer to Table 1 for the X-Ray fluxes determined from these models at each epoch and Fig 3 for the spectra.

3.2. Radio Spectral Fitting

Radio emission from supernovae can be modeled as synchrotron emission from the interaction between supernova ejecta and circumstellar matter (Chevalier 1982). Most radio light-curves show a power-law decline at late times and rise due to low-frequency absorption processes (Weiler et al. 2002) at early times. The rising part has been often modeled as free-free absorption allowing one to estimate the circumstellar density. On the other hand assuming synchrotron self-absorption yields an approximate radius of the emission region at the time of peak flux both for Newtonian (Chevalier 1998) and relativistic (Chakraborti & Ray 2011) explosions. If another mechanism such as free-free absorption is dominant, the radius must be even larger. Chevalier et al. (2006) argue that the expansion velocities of $\sim 10^4 \text{ km s}^{-1}$ implied for the Type IIP supernovae in the synchrotron self-absorption model are similar to those expected for circumstellar interaction and are thus consistent with this absorption mechanism.

We therefore fit the radio spectrum of SN 2011ja with a synchrotron self-absorption model (see Fig 4). The spectral indices of the optically thick and thin parts are fixed to -1 and $5/2$ respectively. The best fit determines the two free parameters, namely the peak flux density ($F_p = 0.829 \pm 0.033 \text{ mJy}$) and the peak frequency ($\nu = 9.29 \pm 0.39 \text{ GHz}$) of the spectrum on 2011 December 19.

4. BLASTWAVE PARAMETERS

We can now use the results of the multi-wavelength observation and analysis described above, to constrain the parameters of the supernova blastwave and its interaction with the circumstellar matter.

4.1. Explosion date

It is important to determine the explosion date of SN 2011ja, so that meaningful comparison with models for circumstellar interaction are possible. Constraining the

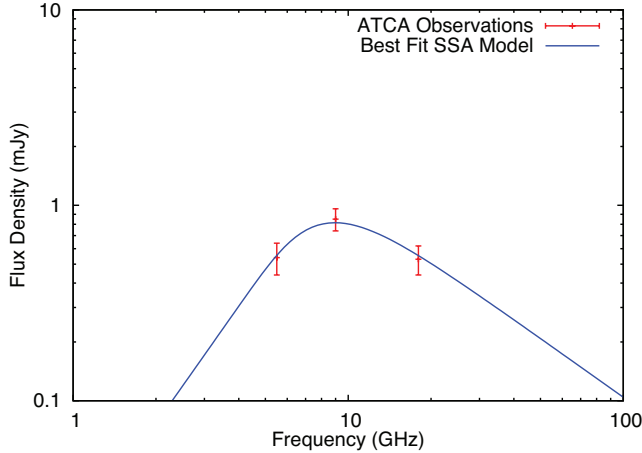


FIG. 4.— Synchrotron self-absorption model fit to the SN 2011ja flux densities observed with the ATCA. Note the optically thin part to the right ($\sim \nu^{-1}$) and the optically thick part to the left ($\sim \nu^{5/2}$).

explosion dates of nearby core collapse supernovae is also important from the perspective of multi-messenger astronomy. For example neutrino detectors have limited direction sensitivity and one would need constraints on the explosion date to discuss the possibility of associating a few (say ~ 2) neutrinos with a nearby supernova.

The forward shock accelerates electrons to relativistic energies. Synchrotron losses from these electrons produce the radio emission from supernovae. Chevalier (1982) modelled the radio emission by assuming that a fraction ϵ_e or ϵ_B of the thermal energy is used to accelerate electrons and amplify magnetic fields respectively. Using this assumption and a self similar blastwave solution Chevalier (1998) derived the radius of the radio emitting region as

$$R_s = 4.0 \times 10^{14} \alpha^{-1/19} \left(\frac{f}{0.5}\right)^{-1/19} \left(\frac{F_p}{\text{mJy}}\right)^{9/19} \times \left(\frac{D}{\text{Mpc}}\right)^{18/19} \left(\frac{\nu}{5 \text{ GHz}}\right)^{-1} \text{ cm}, \quad (1)$$

where F_p is the peak flux at peak frequency ν , the equipartition factor is defined as $\alpha \equiv \epsilon_e/\epsilon_B$ the ratio of relativistic electron energy density to magnetic energy density and f is the fraction of the spherical volume occupied by the radio-emitting region. It can be seen from the equation above that the estimated radius is insensitive to the assumption of equipartition. We therefore use our radio spectrum to estimate a size of $R_s = (1.848 \pm 0.085) \times 10^{15}$ cm.

We further note that Milisavljevic et al. (2011) reported that the absorption minimum of the $H\alpha$ line is found to be blue-shifted by about 11000 km s^{-1} , which is usual for type IIP supernovae. Assuming a 10% uncertainty in the expansion velocity, we get an age of 19.4 ± 2 days at the time of the radio observations. Our best estimate for the explosion date is therefore 2011 November 30 UT (± 2 days). This is consistent with the fact that the optical spectra taken on December 19.1 UT matches best with the spectrum of type IIP event SN 2004et taken about a week after maximum light (Milisavljevic et al. 2011).

4.2. Circumstellar interaction

The forward shock accelerates electrons to relativistic velocities and amplifies magnetic fields, which are responsible for the radio emission from supernovae. The supernova ejecta collides inelastically with the circumstellar matter. The external density is described by a power law profile $\rho \propto r^{-s}$, where $s = 2$ for a steady wind. We therefore have

$$\rho_w = \frac{A}{r^2} \equiv \frac{\dot{M}}{4\pi r^2 v_w}, \quad (2)$$

where \dot{M} and v_w are the mass loss rate and velocity of the wind respectively. Chevalier (1982) sets the normalization of the circumstellar density profile as $A \equiv \dot{M}/(4\pi v_w)$. Chevalier (1982) assumes that a fraction ϵ_e of the thermal energy is used to accelerate electrons while a fraction ϵ_B is used to amplify magnetic fields. Hence these microphysical parameters determine the radio brightness of a supernova, which is not a direct measure of the circumstellar density. Chevalier & Fransson (2006) calculate that that radio emission can constrain

$$S_* \equiv A_* \epsilon_{B-1} \alpha^{8/19} = 1.0 \left(\frac{f}{0.5}\right)^{-8/19} \left(\frac{F_p}{\text{mJy}}\right)^{-4/19} \times \left(\frac{D}{\text{Mpc}}\right)^{-8/19} \left(\frac{\nu}{5 \text{ GHz}}\right)^{-4/19} t_{10}^2, \quad (3)$$

at a time $10 \times t_{10}$ days after explosion. Here $\epsilon_{B-1} \equiv \epsilon_B/0.1$ and $A_* \equiv A/(5 \times 10^{11} \text{ g cm}^{-1})$ is a non-dimensionalized proxy for A defined by Chevalier & Fransson (2006). Our radio spectrum determines $S_* = 1.979 \pm 0.398$.

The electron population that emits radio synchrotron, also inverse Compton scatters optical photons into X-rays. This process dominates the non-thermal part of the X-ray spectrum of type IIP supernovae during the plateau phase (Chakraborti et al. 2012). Chevalier & Fransson (2006) have shown that the inverse Compton flux at 1 keV produced by accelerated electrons with $p = 3$, is given by

$$E \frac{dL_{\text{IC}}}{dE} \approx 8.8 \times 10^{36} \gamma_{\text{min}} S_* \alpha^{11/19} V_4 \times \left(\frac{L_{\text{bol}}(t)}{10^{42} \text{ ergs s}^{-1}}\right) t_{10}^{-1} \text{ ergs s}^{-1}. \quad (4)$$

Here the smallest Lorentz factor for an accelerated electron is γ_{min} and $V_4 = 1.1$ is the expansion velocity in units of 10^4 km s^{-1} at $10 \times t_{10}$ days.

During the first epoch ($t_{10} \sim 1.94$) of Chandra observations, we find the inverse Compton flux density to be $(7.27 \pm 1.50) \times 10^{36} \text{ ergs s}^{-1}$. This gives us the left-hand-side of Equation 4. We use the observed value of $S_* = 1.979$ as found using our radio observations and V_4 (~ 1.1) seen in optical spectra. This gives us

$$\gamma_{\text{min}} \alpha^{11/19} \times \left(\frac{L_{\text{bol}}(t)}{10^{42} \text{ ergs s}^{-1}}\right) \sim 1.55. \quad (5)$$

If the spectrum of accelerated electrons starts from those at rest we would have $\gamma_{\text{min}} = 1$. Following the work by Chevalier & Fransson (2006) in the case of SN 2002ap, we consider relativistic electrons with $\gamma_{\text{min}} \sim 2.5$ and

a bolometric luminosity of 10^{42} ergs s^{-1} as is usual for the plateau phase of type IIP supernovae. This gives us $\alpha \sim 0.44$. This is a direct test of the equipartition assumption which demonstrates that the electrons and magnetic fields are not far from equilibrium.

We can now use the above result, Equation 3 defining S_* and a characteristic value of $\epsilon_B = 0.1$ to constrain the pre-explosion mass loss rate of the progenitor to be

$$\dot{M}\epsilon_{B-1} = (2.7 \pm 0.5) \times 10^{-7} \left(\frac{v_w}{10 \text{ km s}^{-1}} \right) M_\odot \text{ yr}^{-1}, \quad (6)$$

during the last century before explosion. This is smaller than what is expected for typical red supergiant progenitors (see Figure 5) but similar to the mass loss rate seen for the progenitor of SN 2004dj (Chakraborti et al. 2012).

5. TEMPORAL VARIATION

The X-ray spectra of type IIP supernovae, such as SN 2004et (Rho et al. 2007) and SN 2004dj (Chakraborti et al. 2012), soften and fall in luminosity over time. Chakraborti et al. (2012) have shown that at initially, the Compton flux dominated the spectrum and produces a harder spectrum. But the number density of seed photons available for scattering decreases when the optical luminosity from the supernova falls rapidly at the conclusion of the plateau phase. Therefore at late-times the thermal emission from the reverse-shocked plasma dominates the spectrum and makes it softer. We obtained a second epoch of Chandra observations of SN 2011ja to study its temporal variation.

5.1. X-ray rise

The inverse Compton X-ray flux varies in time due to the expansion of the blastwave and the change in the number density of seed photons. If the blastwave encounters circumstellar matter set up by the uniform wind of the progenitor, Chevalier & Fransson (2006) have demonstrated that the inverse Compton flux varies as

$$E \frac{dL_{IC}}{dE} \propto \frac{L_{bol}(t)}{t}. \quad (7)$$

Therefore during the plateau phase of a type IIP supernova when there is a nearly constant L_{bol} the inverse Compton flux should be $\propto t^{-1}$. Since the supernova is likely ~ 125 days old during the second epoch of Chandra observations, one would expect an X-ray flux reduced by at least a factor of ~ 6.4 . Instead we find an increase in flux by a factor of ~ 4.2 . This is inconsistent with the predictions assuming a circumstellar density $\propto r^{-2}$ set up by a steady wind. Unless micro-physical parameters such as the efficiency of electron acceleration ϵ_e changed between the two epochs, this implies a variable mass loss rate for the progenitor. A similar rise was reported by Pooley et al. (2002) for SN 1999em at around ~ 100 days after explosion, where the total flux nearly doubled from the previous observation, despite the continued decline of the high-energy X-rays. Therefore the spectra softened remarkably during the sudden rise in flux. For SN 2011ja, the Chandra X-ray source hardness ratio, calculated as $(H - S)/(H + S)$ where S and H are the counts in the 0.5 to 2 keV band and the 2 to 8 keV band respectively, changes from 0.08 ± 0.20 to 0.10 ± 0.10 which is consistent with no change between ~ 41 and ~ 84 days after

explosion. If the increase in X-ray flux resulted from increased circumstellar interaction, then the inverse Compton component should scale as $\propto \dot{M}$ while the thermal component should scale as $\propto \dot{M}^2$, eventually overtaking the former for a mass loss rate of $\sim 10^{-5} M_\odot \text{ yr}^{-1}$. The hardness ratio should have changed if for example thermal emission from the reverse shocked plasma started to dominate or if the absorption column got reduced. Therefore the emission continues to be dominated by the non-thermal inverse Compton component. This is confirmed by our exploration of the model parameter space following the MCMC method outlined in Section 3.1.

5.2. Density enhancement

The supernova ejecta moves a thousand times faster than typical red supergiant winds and probes three centuries of mass loss history during the period spanned by our observations. This potentially offers us a glimpse into the last stages of stellar evolution before core collapse. Inverse Compton flux scales directly with the number of seed photon (roughly constant during the plateau), mass loss rate and inversely with time. Therefore we argue that one needs an enhanced density by a factor of ~ 27 to account for the increased flux in the second epoch. We find a mass loss rate of

$$\dot{M}\epsilon_{B-1} = (7.5 \pm 1.5) \times 10^{-6} \left(\frac{v_w}{10 \text{ km s}^{-1}} \right) M_\odot \text{ yr}^{-1}. \quad (8)$$

However, this calculation is based on the scaling relation given in Eq. 4, which was derived from the self similar solution of Chevalier (1982), assuming a steady wind. In Eq. 4 the emission is also a function of the shock velocity, so if the supernova slowed down significantly between the two epochs, then it will increase the density enhancement required. Therefore, while the argument is physically well-grounded, the result can be incorrect by a factor of a few. This should motivate investigations into the propagation of supernova blastwaves into environments with density jumps. One such situation could be the evolution of supernovae in circumstellar wind-blown bubbles explored by Dwarkadas (2005).

6. DISCUSSION

The results presented here tell us about the circumstellar environments of the progenitors of type IIP supernovae and the equipartition assumption often invoked in supernovae shocks. These are explored in brief below.

6.1. Equipartition in radio supernovae

Radio emission from non-thermal sources can be explained with various amounts of accelerated electrons and amplified magnetic fields (Pacholczyk 1970). It is however difficult to constrain the relative contribution of each. Burbidge (1956) demonstrated that assuming minimum energy in the emission region, implies that these energy densities are approximately in equipartition. Scott & Readhead (1977) observed that for sources having low-frequency spectral turnovers, the total energy is within a factor of a few of the equipartition energy. Kulkarni et al. (1998) used the equipartition argument to estimate the radius expansion of the GRB associated SN 1998bw. Chevalier (1998) noted that the inferred radii of synchrotron self absorbed sources are insensitive to the assumption of equipartition. Therefore independent

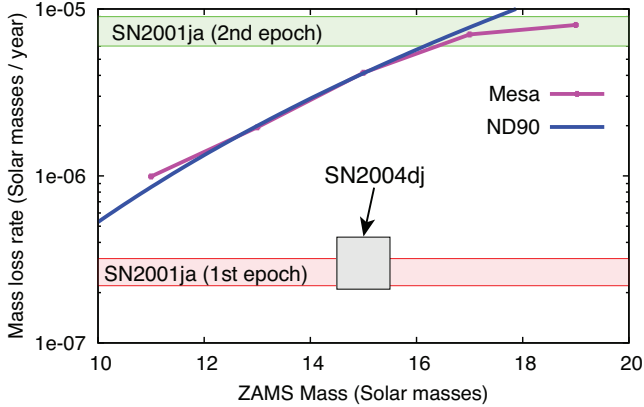


FIG. 5.— Zero Age Main Sequence Mass (ZAMS) and wind mass loss rate (during the last 100 years of stellar evolution) for MESA runs (magenta), and theoretical line (blue) from Nieuwenhuijzen & de Jager (1990) (with $R = 10^3 R_{\odot}$) plotted for comparison. Shaded boxes are 1σ confidence intervals for the mass loss rate observed in SN 2011ja (corresponding to $\epsilon_B = 0.1$) first epoch (red), second epoch (green) and SN 2004dj from Chakrabarti et al. (2012) (grey). There is disagreement between the predicted and observed mass loss rate of the SN 2011ja progenitor during the first epoch and the subsequent agreement during the second epoch.

size measurements do not tightly constrain the equipartition parameter α . Chandra et al. (2004) have suggested looking for a spectral break so that the magnetic field and the size of the radio-emitting region are determined through unrelated methods.

Using SN 2004dj as a prototype Chakrabarti et al. (2012) have demonstrated that if the inverse Compton scattered supernova photons can be detected in the X-rays along with radio synchrotron emission, the parameters of the system can be derived without the help of the equipartition argument. Soderberg et al. (2012) has explained the radio and X-ray properties of SN 2011dh using the synchrotron and inverse Compton mechanisms respectively with a $\alpha \sim 30$ while Maeda (2012) finds $\alpha \lesssim 1$ and Horesh et al. (2012) find $\alpha \sim 1000$. Barniol Duran et al. (2013) have similarly shown that for sources where the Synchrotron-self-Compton component can be identified, the equipartition argument is not necessary. In this work, by comparing the radio synchrotron and X-ray inverse Compton flux densities, we have determined the equipartition factor for SN 2011ja. Our result shows that the plasma in SN 2011ja is indeed close to equipartition.

6.2. Progenitors of type IIP Supernovae

Massive stars ($M \gtrsim 8M_{\odot}$) evolve from a main sequence blue giant to a red supergiant and then explode as supernovae. Such a sequence of events is consistent with observations of most type IIP supernovae, their progenitors and circumstellar interaction. Here we compare the observed mass loss rates of the progenitor of SN 2011ja, with those of its expected progenitors. MESA (Paxton et al. 2011) was used to evolve stars with masses between 11 to 19 M_{\odot} , for a metallicity of $z = 0.5Z_{\odot}$. (Paxton et al. 2011) Sec 6.6 describe the mass loss prescription used in our simulations as the *Dutch Scheme*. This prescription turns on a RGB wind at the correct burning stage. Changes in surface temperatures in different evolutionary stages are also taken into ac-

count. The supernova ejecta encounters the mass lost during the RGB phase which follows the prescription from de Jager et al. (1988). We evolved the stars until they reached a central density of $10^{12} \text{ g cm}^{-3}$. We averaged the mass loss over the final hundred years to obtain our fiducial values. The supernova ejecta should encounter this circumstellar matter over the first months after explosion.

The results of the above simulation are compared with the observations in Figure 5. For this comparison, recall that with time circumstellar interaction probes deeper into the progenitor’s mass loss history. Note that the circumstellar density observed in the first epoch, corresponding to the final stage of mass loss before core collapse, is far below expected values for red supergiant progenitors. Chugai et al. (2007) also noted a similar disagreement for mass loss rates obtained from optical spectroscopy of SN 1999em and SN 2004dj. Similar values are derived by Chakrabarti et al. (2012) for the mass loss rate of SN 2004dj from X-ray spectroscopy. Note however that by the second epoch of observations, corresponding to an earlier stage of the progenitor star’s life, the mass loss is consistent with that from a red supergiant of $M \gtrsim 16M_{\odot}$. Similarly, Kochanek et al. (2012) have used X-ray observations of SN 2012aw to infer a varying mass loss rate.

The mass loss rate implied by Eq. 6 is very low for a slow moving red supergiant wind, but not for a fast moving wind of a blue giant. At the same mass loss rate, a faster wind sets up a lower circumstellar density. For example, the progenitor of SN 1987A was identified to be a blue giant (Arnett et al. 1989, and references therein). The circumstellar environment of a red supergiant is set up by its slow and dense stellar wind. However, if the star becomes a blue giant again before it undergoes core collapse, it will blow a hot low density bubble within the red supergiant wind. In such a situation, the supernova remnant will encounter little circumstellar matter at early times but have stronger interaction subsequently. This is indeed consistent with our observation and analysis of SN 2011ja. Such an interaction was predicted by Chevalier & Liang (1989) for SN 1987A, while Luo & McCray (1991) predicted a sharp rise in radio and X-ray luminosities. This rise was subsequently observed by Staveley-Smith et al. (1992).

Bauer et al. (2008) have suggested that a similar situation can explain the observations of the exotic type II_n SN 1996cr. Dwarkadas et al. (2010) studied the increasing X-ray flux from SN 1996cr, using a hydrodynamical model, computing non-equilibrium ionization spectra and light curves, then fitting them to observations, to fully understand the circumstellar environment. Circumstellar interaction in this and other (Chandra et al. 2012) type II_n have received recent attention. Ofek et al. (2013) have observed of a remarkable mass-loss event detected 40 days prior to the explosion of the Type II_n supernova SN 2010mc. Radio and X-ray observations of SN 2003bg (Soderberg et al. 2006), the ordinary type Ic SN 2007gr (Soderberg et al. 2010) and the broad-lined type Ic SN 2007bg (Salas et al. 2013) have revealed their complex circumstellar environments. Wellons et al. (2012) have explored the unusual circumstellar environments for type Ibc Supernovae 2004cc, 2004dk and 2004gq. The peculiar SN 1987A is also interacting with a complex cir-

cumstellar environment (Dewey et al. 2012). Compared to type II_n and type Ibc supernovae, few type IIP supernovae have had their environments studied in detail like Supernovae 1999em (Pooley et al. 2002) and 2004et (Misra et al. 2007). Here we suggest that the regular type IIP SN 2011ja is undergoing interaction with a complex circumstellar environment set up by a non-steady wind.

7. CONCLUSIONS

Radio and X-ray observations of SN 2011ja allow us to measure micro-physical parameters such as the ratio of energies which goes into accelerating electrons and amplifying magnetic fields. It is deduced that in this case, the plasma is not far from equipartition which is often assumed in the study of supernova circumstellar interaction. Radio observations have allowed us to constrain the date of explosion. Multiple epochs of Chandra observations have allowed us to demonstrate that the supernova initially encountered a low density region, inconsistent with the expected mass loss rate of a red supergiant progenitor. The fast moving ejecta subsequently catches up to the slowly moving wind from a possibly $M_{\text{ZAMS}} \gtrsim 16M_{\odot}$ red supergiant. This interaction with a lower density region followed by stronger circumstellar interaction is consistent with a SN 1987A-like blue giant progenitor with a fast wind for SN 2011ja and indicates that a fraction of type IIP supernovae may happen inside circumstellar bubbles blown by hot progenitors or with complex circumstellar environments set up by variable winds. If a rise at ~ 100 days in X-ray fluxes as seen in SN 1999em (Pooley et al. 2002) and SN 2011ja (this work) is more common than expected, multiple Chandra observations of young nearby type IIP supernovae

are needed in the first year after explosion. In such a situation, for studies of circumstellar interaction of type IIP supernovae, optical (Chugai et al. 2007), radio and X-ray (Chevalier et al. 2006) spectra at multiple epochs, are necessary to constrain the environments and progenitors of type IIP supernovae.

This research has made use of data obtained using the Chandra X-ray Observatory through an advance Target of Opportunity program and software provided by the Chandra X-ray Center (CXC) in the application packages CIAO and ChIPS. We thank CXC Director Harvey Tananbaum for the second epoch of Chandra observation which was made possible using the Director's Discretionary Time. The ATCA is part of the Australia Telescope National Facility which is funded by the Commonwealth of Australia for operation as a National Facility managed by CSIRO. We thank the staff of the GMRT that made GMRT observations possible. GMRT is run by the National Centre for Radio Astrophysics of the Tata Institute of Fundamental Research. Support for this work was provided by the National Aeronautics and Space Administration through Chandra Award Number 13500809 issued by the Chandra X-ray Observatory Center, which is operated by the Smithsonian Astrophysical Observatory for and on behalf of the National Aeronautics Space Administration under contract NAS8-03060. AR thanks the Department of Physics at West Virginia University for hospitality and the Twelfth Five Year Plan Program 12P-407 at TIFR. NY is supported by the CSIR S.P. Mukherjee Fellowship.

REFERENCES

- Arcavi, I., et al. 2012, *ApJ*, 756, L30
 Arnett, W. D., Bahcall, J. N., Kirshner, R. P., & Woosley, S. E. 1989, *ARA&A*, 27, 629
 Barniol Duran, R., Nakar, E., & Piran, T. 2013, *ArXiv e-prints*
 Bauer, F. E., Dwarkadas, V. V., Brandt, W. N., Immler, S., Smartt, S., Bartel, N., & Bietenholz, M. F. 2008, *ApJ*, 688, 1210
 Björnsson, C.-I., & Fransson, C. 2004, *ApJ*, 605, 823
 Burbidge, G. R. 1956, *ApJ*, 124, 416
 Cash, W. 1979, *ApJ*, 228, 939
 Chakraborti, S., & Ray, A. 2011, *ApJ*, 729, 57
 Chakraborti, S., Yadav, N., Ray, A., Smith, R., Chandra, P., & Pooley, D. 2012, *ApJ*, 761, 100
 Chandra, P., Chevalier, R. A., Chugai, N., Fransson, C., Irwin, C. M., Soderberg, A. M., Chakraborti, S., & Immler, S. 2012, *ApJ*, 755, 110
 Chandra, P., Ray, A., & Bhatnagar, S. 2004, *ApJ*, 612, 974
 Chevalier, R. A. 1982, *ApJ*, 258, 790
 —. 1998, *ApJ*, 499, 810
 Chevalier, R. A., & Fransson, C. 2006, *ApJ*, 651, 381
 Chevalier, R. A., Fransson, C., & Nymark, T. K. 2006, *ApJ*, 641, 1029
 Chevalier, R. A., & Liang, E. P. 1989, *ApJ*, 344, 332
 Chugai, N. N., Chevalier, R. A., & Utrobin, V. P. 2007, *ApJ*, 662, 1136
 Crockett, R. M., Smartt, S. J., Pastorello, A., Eldridge, J. J., Stephens, A. W., Maund, J. R., & Mattila, S. 2011, *MNRAS*, 410, 2767
 de Jager, C., Nieuwenhuijzen, H., & van der Hucht, K. A. 1988, *A&AS*, 72, 259
 Dewey, D., Dwarkadas, V. V., Haberl, F., Sturm, R., & Canizares, C. R. 2012, *ApJ*, 752, 103
 Doggett, J. B., & Branch, D. 1985, *AJ*, 90, 2303
 Dwarkadas, V. V. 2005, *ApJ*, 630, 892
 Dwarkadas, V. V., Dewey, D., & Bauer, F. 2010, *MNRAS*, 407, 812
 Dwarkadas, V. V., & Gruszko, J. 2012, *MNRAS*, 419, 1515
 Horesh, A., et al. 2012, *ArXiv e-prints*
 Jerkstrand, A., Fransson, C., Maguire, K., Smartt, S., Ergon, M., & Spyromilio, J. 2012, *A&A*, 546, A28
 Kochanek, C. S., Khan, R., & Dai, X. 2012, *ApJ*, 759, 20
 Kulkarni, S. R., et al. 1998, *Nature*, 395, 663
 Luo, D., & McCray, R. 1991, *ApJ*, 372, 194
 Maeda, K. 2012, *ApJ*, 758, 81
 Milisavljevic, D., Fesen, R., Pickering, T., Romero-Colmenero, E., Sodeberg, A., & Margutti, R. 2011, *Central Bureau Electronic Telegrams*, 2946, 2
 Misra, K., Pooley, D., Chandra, P., Bhattacharya, D., Ray, A. K., Sagar, R., & Lewin, W. H. G. 2007, *MNRAS*, 381, 280
 Monard, L. A. G., et al. 2011, *Central Bureau Electronic Telegrams*, 2946, 1
 Moriya, T. J. 2012, *ApJ*, 750, L13
 Mouhcine, M., Ferguson, H. C., Rich, R. M., Brown, T. M., & Smith, T. E. 2005, *ApJ*, 633, 810
 Nieuwenhuijzen, H., & de Jager, C. 1990, *A&A*, 231, 134
 Nymark, T. K., Fransson, C., & Kozma, C. 2006, *A&A*, 449, 171
 O'Connor, E., & Ott, C. D. 2011, *ApJ*, 730, 70
 Ofek, E. O., et al. 2013, *Nature*, 494, 65
 Pacholczyk, A. G. 1970, *Radio astrophysics. Nonthermal processes in galactic and extragalactic sources*
 Paxton, B., Bildsten, L., Dotter, A., Herwig, F., Lesaffre, P., & Timmes, F. 2011, *ApJS*, 192, 3
 Pooley, D., et al. 2002, *ApJ*, 572, 932
 Popov, D. V. 1993, *ApJ*, 414, 712
 Rho, J., Jarrett, T. H., Chugai, N. N., & Chevalier, R. A. 2007, *ApJ*, 666, 1108

- Ryder, S., Soderberg, A., Stockdale, C., van Dyk, S., Immler, S., Weiler, K., & Panagia, N. 2011, Central Bureau Electronic Telegrams, 2946, 4
- Sahu, D. K., Anupama, G. C., Srividya, S., & Muneer, S. 2006, MNRAS, 372, 1315
- Salas, P., Bauer, F. E., Stockdale, C., & Prieto, J. L. 2013, MNRAS, 428, 1207
- Sault, R. J., Teuben, P. J., & Wright, M. C. H. 1995, in Astronomical Society of the Pacific Conference Series, Vol. 77, Astronomical Data Analysis Software and Systems IV, ed. R. A. Shaw, H. E. Payne, & J. J. E. Hayes, 433
- Scott, M. A., & Readhead, A. C. S. 1977, MNRAS, 180, 539
- Smartt, S. J., Eldridge, J. J., Crockett, R. M., & Maund, J. R. 2009, MNRAS, 395, 1409
- Smith, N., Li, W., Filippenko, A. V., & Chornock, R. 2011, MNRAS, 412, 1522
- Smith, R. K., Brickhouse, N. S., Liedahl, D. A., & Raymond, J. C. 2001, ApJ, 556, L91
- Soderberg, A. M., Brunthaler, A., Nakar, E., Chevalier, R. A., & Bietenholz, M. F. 2010, ApJ, 725, 922
- Soderberg, A. M., Chevalier, R. A., Kulkarni, S. R., & Frail, D. A. 2006, ApJ, 651, 1005
- Soderberg, A. M., et al. 2012, ApJ, 752, 78
- Staveley-Smith, L., et al. 1992, Nature, 355, 147
- Sutaria, F. K., Chandra, P., Bhatnagar, S., & Ray, A. 2003, A&A, 397, 1011
- Walmswell, J. J., & Eldridge, J. J. 2012, MNRAS, 419, 2054
- Weiler, K. W., Panagia, N., Montes, M. J., & Sramek, R. A. 2002, ARA&A, 40, 387
- Weiler, K. W., Panagia, N., Stockdale, C., Rupen, M., Sramek, R. A., & Williams, C. L. 2011, ApJ, 740, 79
- Wellons, S., Soderberg, A. M., & Chevalier, R. A. 2012, ApJ, 752, 17
- Wilms, J., Allen, A., & McCray, R. 2000, ApJ, 542, 914
- Wilson, W. E., et al. 2011, MNRAS, 416, 832
- Yadav, N., & Chakraborti, S. 2012, The Astronomer's Telegram, 3899, 1